Rhythmic Growth-Induced Concentric Ring-Banded Structures in Poly(ϵ-caprolactone) Solution-Casting Films Obtained at the Slow Solvent Evaporation Rate

Zongbao Wang,[†] Zhijun Hu,[‡] Yongzhong Chen,[†] Yumei Gong,[†] Haiying Huang,[†] and Tianbai He*,[†]

State Key Laboratory of Polymer Physics and Chemistry, Changchun Institute of Applied Chemistry, Graduate University of Chinese Academy of Sciences, Chinese Academy of Sciences, Changchun 130022, P. R. China, and Laboratoire de Chimie et de Physique des Hauts Polyme'res (POLY), UniVersite' catholique de LouVain, Place Croix du Sud 1, B-1348 LouVain-la-NeuVe, Belgium

Received February 7, 2007
Revised Manuscript Received April 8, 2007

Introduction

Ring-banded structures are often observed in some semicrystalline homopolymers[1−5] and polymer blends[6−8] melt crystallized in polymer bulk and films. It is generally believed that the formation of ring-banded structures is attributed to periodic twisting of lamellar crystals along the radial growth direction of the spherulites.[9−15] On the basis of simulation, however, Kyu et al.[16] proposed that the twisting of lamellar crystals might not be the only reason for the formation of ring-banded structures, that the concentric ring-banded structures might be a consequence of rhythmic crystal growth resulting from nonlinear diffusion during growth. Generally speaking, rhythmic crystal growth may be encountered in thin films because of the mass and spatial confinement.[17] Rhythmic crystal growth of ring-banded structures has been observed experimentally in some crystalline/amorphous polymer blends[18,19] and crystalline/crystalline polymer blends.[20,21] Recently, Schultz et al.[22,23] reported nonbirefringent concentric ring-banded structures consisting of multilayer polymer lamellar crystals with the chain axis normal to the film plane in isotactic polystyrene thin films. It was considered that the alternating ridge and valley bands were derived from rhythmic crystal growth as a result of the inability of the molten polymer diffusion to keep up with the growth of crystals. Very recently, Chan et al.[24] observed concentric ring-banded structures with the chain axis uniformly normal to the film plane by AFM observations in thin poly(bisphenol A hexane ether) films. It is worth mentioning at this point that all the results that have been published in literature concerning rhythmic crystal growth of ring-banded structures were observed only from melt crystallization.

In previous studies,[25] by controlling the solvent evaporation rate during polymer solution casting, we obtained a large quantity of uniformly distributed poly(di-*n*-butylsilane) single crystals of all-trans conformation, which had been observed only under extreme conditions before.[26] In this study, we adopt the same approach to explore poly(ϵ-caprolactone) (PCL) ring-banded structures by controlling the kinetics process of solvent evaporation in solution-casting film. A concentric ring-banded spherulite with the chain axis normal to the film plane is obtained at the slow solvent evaporation rate, and the rhythmic growth mechanism caused by periodically changing concentration gradient is discussed.

* To whom all correspondence should be addressed: e-mail tbhe@ciac.jl.cn; Fax +86-431-85262126; Tel +86-431-85262123.
[†] Chinese Academy of Sciences.
[‡] UniVersite' catholique de LouVain.

Experimental Part

The PCL used in this work was purchased from Polysciences Inc., with a number-average molecular weight of 11 300 g/mol and a polydispersity index (M_w/M_n) of 1.95 determined by gel permeation chromatography (GPC). The purchased product was purified by dissolving it in chloroform and precipitating into methyl alcohol, followed by centrifugation and drying in a vacuum at room temperature for 24 h. The obtained pure white PCL powder was dissolved in toluene at room temperature and in the absence of light for at least 24 h to produce solution with concentration of 5 mg/mL. Before use, the solution was heated to 80 °C for 30 min to dissolve any crystals that might form when the solution was kept for long time at room temperature. 10 μL solution was cast onto cleaned silicon wafers (p-type single-side polished (100) silicon wafers) inside a cylinder container with radius and height 1.0 and 2.5 cm, respectively, at room temperature. The solvent evaporation rate was controlled by adding different volumes of extra toluene solvent to the container covered with a lid or by uncovering the lid. The solvent evaporation rate was measured by weighing the container at different selected times. A slow solvent evaporation rate of 1.5×10^{-4} mL/h was achieved by adding 200 μL of extra toluene solvent to the container covered with a lid. Under these conditions, solvent can only escape through the small gap between the container and its lid. Extra toluene solvent placed in the container generated a toluene partial pressure to slow down the solvent evaporation from PCL solution. The evaporation of solvent in the container was complete after ca. 4 days for the container maintained at 20 °C.

The optical microscopy (OM) observations of the thin films were performed using a Leica DMLP microscope equipped with a CCD camera. The atomic force microscopy (AFM) studies were performed with a SPA-300HV atomic force microscope with an SPI 3800N controller (Seiko Instruments Industry Co., Ltd.). Probes with resonant frequency of 250−300 kHz and spring constants of 42 N/m were used. A 150 μm scanner was selected, and the tapping mode was used to obtain height and phase images. Transmission electronic microscopy (TEM) experiments were performed using a JEOL JEM 1011 TEM with an accelerating voltage of 100 kV for bright field (BF) and electron diffraction (ED) modes.

Results and Discussion

The global morphology of the concentric ring-banded spherulites was investigated by OM. Figure 1 shows two OM images of PCL concentric ring-banded spherulites formed at the solvent evaporation rate of 1.5×10^{-4} mL/h from 5 mg/mL toluene solution at 20 °C. Figure 1a was obtained under crossed-polarized light, and nonbirefringent regularly spaced concentric ring-banded structures can be seen. While under unpolarized light (Figure 1b), the concentric ringed-banded structures are seen even more clearly. In addition, there are inner rings and radial irregular features as shown in Figure 1b. It is worth mentioning at this point that the radii of inner rings of different spherulites are approximately equal.

The details of the concentric ring-banded spherulites were investigated by AFM. A typical AFM topography image is shown in Figure 2a. The height profile along the added black line is shown in Figure 2b. The above two images reveal more clearly the concentric periodic ringed-banded structures. It can be easily observed that alternating ridges and valleys are the source of the concentric ring bands. The band spacing was

10.1021/ma070334+ CCC: $37.00
Published on Web 05/16/2007

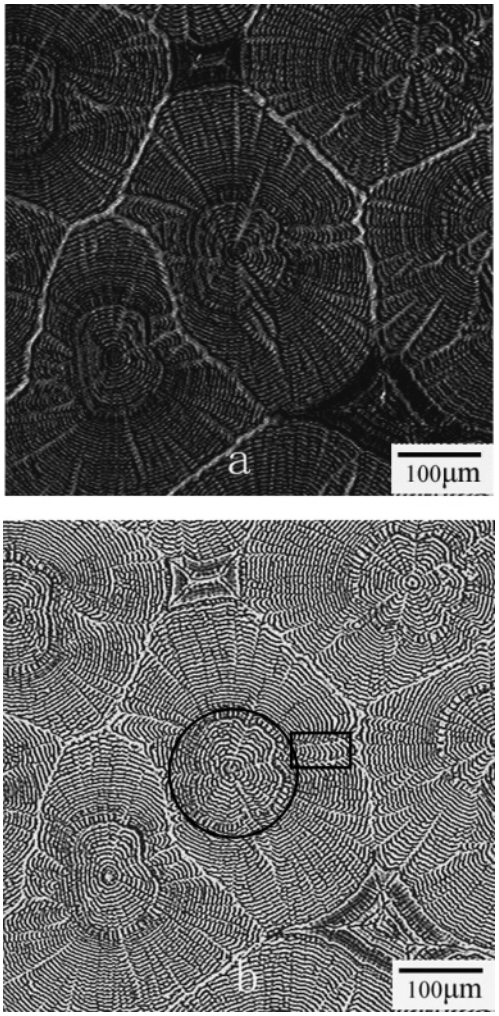

Figure 1. OM images of PCL concentric ring-banded spherulites formed at the solvent evaporation rate of 1.5×10^{-4} mL/h from 5 mg/mL toluene solution at 20 °C with inner ring shown by the black circle and radial irregular features shown by the black square: (a) taken under crossed-polarized light; (b) taken under unpolarized light.

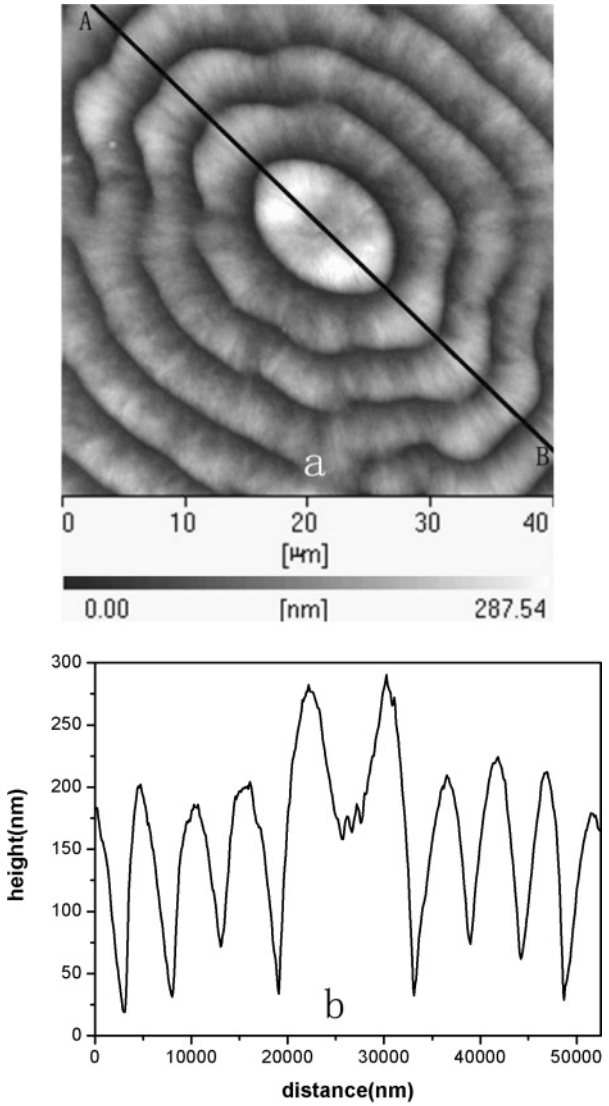

Figure 2. (a) AFM height image of PCL concentric ring-banded spherulites formed at the solvent evaporation rate of 1.5×10^{-4} mL/h from 5 mg/mL toluene solution at 20 °C. (b) The corresponding height profile line of the through-diameter trace between A and B shown in (a).

calculated as 5.46 ± 0.56 μm. The height profile in Figure 2b shows further intriguing details: the central crystals are much higher than the bands around, and the figure of height profile is similar between the central crystals and the bands around. In addition, the height increases slowly toward the ridge but decreases sharply into the valley of a band.

The structures of the concentric ring-banded spherulites were further investigated by TEM. Figure 3 shows BF images and ED patterns of the PCL concentric ring-banded spherulites formed at the solvent evaporation rate of 1.5×10^{-4} mL/h from 5 mg/mL toluene solution at 20 °C. The alternating bright and dark bands in Figure 3a correspond to the valleys and ridges of AFM height image (Figure 2a), respectively. Figure 3b shows the ED pattern of the bright band in Figure 3a in the location shown by the dark circle. Figure 3c shows the ED pattern of the dark band in Figure 3a in the location shown by the white circle. All of the diffraction spots can be indexed on the basis of orthorhombic packing of the PCL crystal.[27,28] The strong (*hk*0) diffraction patterns indicate that the PCL molecular chains (*c*-axes) of alternating ridge and valley bands are normal to the film plane, with the *a*- and *b*-axes in the film plane. Moreover, the {*h*00} planes accord with the radial growth direction of concentric ring-banded spherulites, which indicates that crystallographic *b*-axes coincide with the radial direction. It should be pointed out that the ED patterns have been taken in various regions of ring bands, and the results at all positions are almost identical with those mentioned above. The results above suggest that the alternating ridge and valley bands are stacks of lamellar crystals with the polymer chains (*c*-axes) normal to the film plane and growth direction (*b*-axes) coincident with the radial direction.

Unambiguously, this kind of concentric ring-banded structures is different from classical ring-banded structures, and a nonlinear diffusion-induced rhythmic growth process caused by periodically changing concentration gradient is suggested. The formation process is analogous to the development of Liesegang rings, which have been well-known for a long time in small molecule systems.[29] The concentric ring-banded spherulites growth reflects the competition between the polymer chains diffusion flux in solution J and the spherulites growth velocity in the radial direction V. This competition can be characterized by a parameter $\delta = J/V$, a measurement of the per unit volume quantity that polymer chains diffuse to the crystallization front. The formation of alternating ridge and valley bands is owing to that the diffused polymer chains are enough for the ridge bands and insufficient for the valley bands. The imbalance of

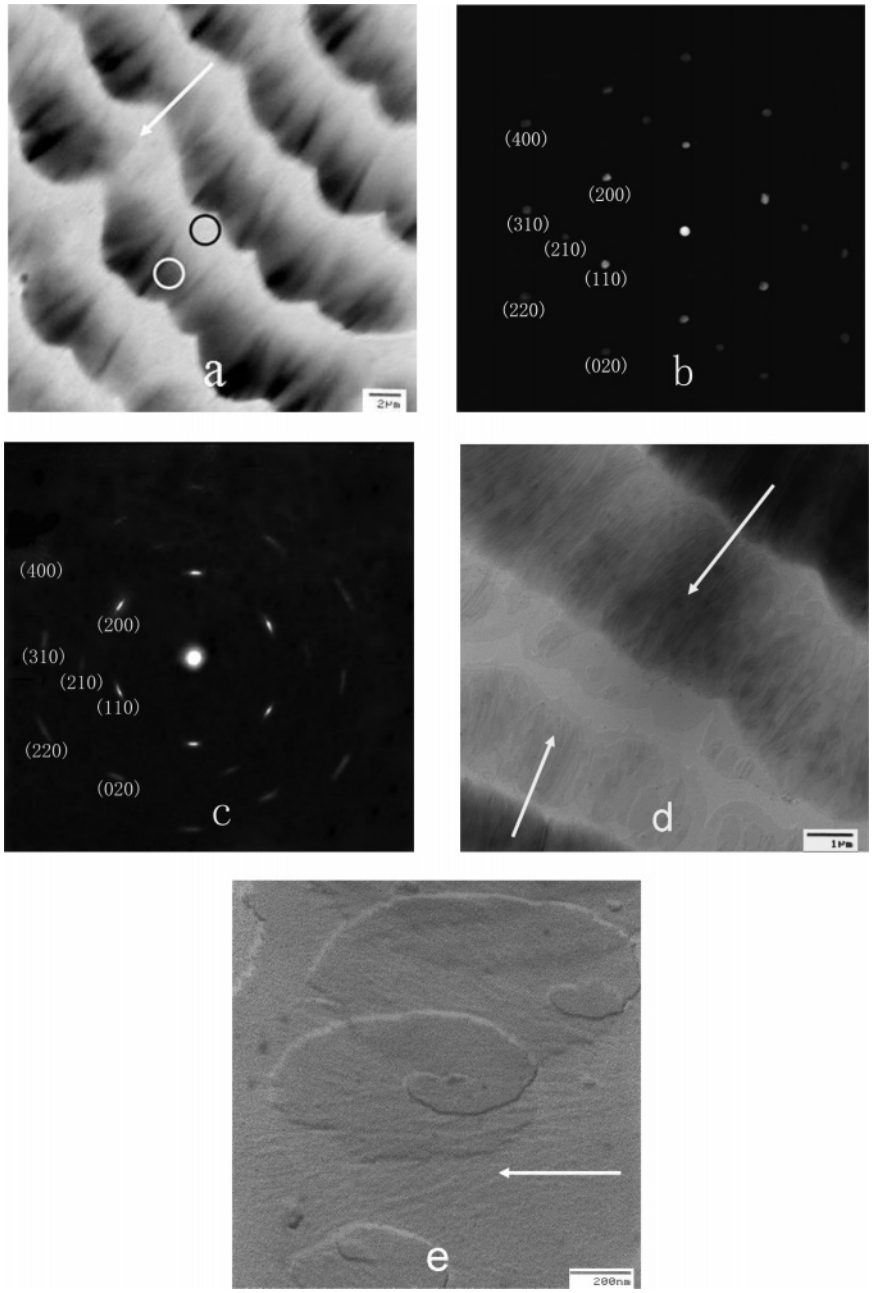

Figure 3. (a) BF image of the PCL concentric ring-banded spherulites formed at the solvent evaporation rate of 1.5×10^{-4} mL/h from 5 mg/mL toluene solution at 20 °C, with the radial growth direction shown by the arrow. (b) ED pattern of the bright band in (a) in the location shown by the black circle. (c) ED pattern of the dark band in (a) in the location shown by the white circle. (d) BF image of the boundary of two PCL concentric ring-banded spherulites (the spherulite at the top right corner is that shown in (a)), with the radial growth direction shown by the arrows. (e) BF image of the lamellar crystals at the growth front of the PCL concentric ring-banded spherulites, with the radial growth direction shown by the arrows.

supply and demand results in the periodical change of diffused polymer chains quantity and the rhythmic growth of spherulites.

The whole system is a continuous solution phase with a more or less smooth surface, and the polymer chains uniformly distribute in the solution. By controlling the solvent evaporation rate, the velocity that polymer chains separate out from the solution system in the form of concentric ring-banded spherulites matches the velocity that solvent evaporates from the solution system at the slow solvent evaporation rate of 1.5×10^{-4} mL/h. So the concentration of whole polymer solution system, that is, the polymer solution concentration at large distances from the spherulites ϕ_∞, is approximately unchanged during the growth of spherulites. The polymer concentration around the tall central ridge initially has the same value ϕ_∞, but adjustments would later take place in response to the growth of tall central ridge to a lower value ϕ_0 because the transported polymer chains are much insufficient for the continual growth of tall central ridge bands. ϕ_0 is an approximately constant concentration value (much smaller than ϕ_∞) that can accommodate exactly the growth of valley bands. Therefore, the polymer chains transportation would occur between points at which $\phi = \phi_\infty$ and points of $\phi = \phi_0$ because of radial concentration difference. Around the growing spherulites there is a substantial region in which concentration difference is small (and, at some point, actually zero), and the spherulites are "nourished" mainly from the region, which is similar to the depletion zone for melt crystallization. Assuming that the polymer chains transport a distance of l, the radial concentration gradient is represented as the following relationship: $G = (\phi_\infty - \phi_0)/l$. It can be seen from the relation that the concentration gradient G is in inversely

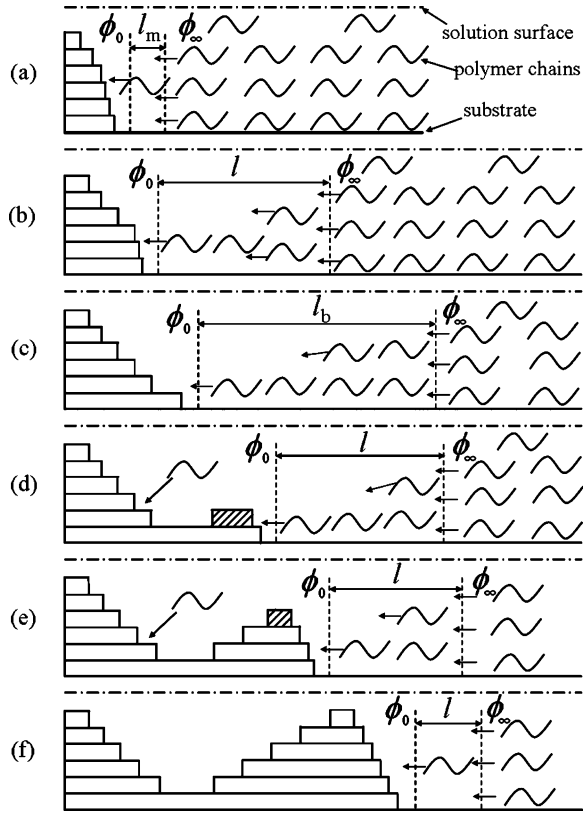

Figure 4. Model of PCL concentric ring-banded spherulites formation (a) at ridge of band; transported distance l is the shortest; concentration gradient G is the largest. (b) Transported distance l increase gradually; concentration gradient G fall gradually; top crystals cannot grow; height decreases sharply. (c) At valley of band; transport distance l increase to the longest; concentration gradient G fall to the smallest; growth of most layers has stopped. (d) Climbing from valley; new lamellar layers are initiated via screw dislocation (hatched); transport distance l decrease gradually; concentration gradient G increase gradually. (e) Lamellar crystals grow upward and forward; climbing further from valley to ridge. (f) The band climbs up to the ridge.

proportional to transported distance l because ϕ_∞ and ϕ_0 are approximately invariable. We assume that polymer chains transportation cannot occur when l increases to a big value l_b; in the present case the polymer chains in front of spherulites can only accommodate the growth of valley bands. L should be self-adjusting periodically between l_b and the minimal value l_m according to the dynamics of the spherulites growth process. Thereby G changes periodically, adapting itself to the needs of the spherulites growth process at every stage. According to Fick's first diffusion law, J changes periodically with the varying concentration gradient during growth, while the concentric ring-banded spherulites growth velocity in the radial direction V is constant in the solution system (1.98 nm/s), as expected from interface kinetics models of Lauritzen and Hoffman.[30] Therefore, the per unit volume quantity δ that polymer chains diffuse to the crystallization front changes periodically during the growth of spherulites. Just the nonlinear diffusion resulting from periodically changing concentration gradient leads to the formation of concentric ring-banded structures. On the basis of the above analysis, the development process of the concentric ring-banded structures in PCL solution-casting films is described using a sequence of schematic diagrams shown in Figure 4. Repeating the rhythmic growth process periodically as described in Figure 4, the concentric ring-banded structures are produced.

It is worth mentioning at this point that the asymmetry of the bands is attributed to the formation of new crystal layers via screw dislocations, as can be seen in Figure 3e. The generation of screw dislocations is a kinetic phenomenon and should occur, on average, only after the underlying crystal has grown forward to some extent.[31] As shown in Figure 4d,e, the concentration gradient increase fast during the formation of screw dislocations because the quantity of transported polymer chains is much overabundant for the growth of crystal layers. Conversely, the increasing concentration gradient more initiates the growth of new lamellar layers via screw dislocations.

To further understand how the concentric ring-banded structures are formed, we studied the effects of initial solution concentration, which have significant influence on the diffuse flux of polymer chains J. PCL concentric ring-banded structures were also obtained from solution-casting films formed at the same solvent evaporation rate of 1.5×10^{-4} mL/h at 20 °C from toluene solution with the corresponding initial solution concentration of 10, 20, and 50 mg/mL. According to the rhythmic growth mechanism proposed above, ϕ_0 is approximately same in different initial concentration solutions, and ϕ_∞ is approximately identical with the initial solution concentration. Consequently, polymer chains in concentrated solution have larger flux J, and chains can transport longer distances l because of larger concentration gradient G. But the crystals growth velocity along the substrate V can be considered changeless compared with the change of concentration gradient G. Therefore, with the increase of initial solution concentration from 5 mg/mL to 10, 20, 50 mg/mL band spacing increases correspondingly from 5.46 μm to 18.6, 31.4, 46.8 μm.

The evidence that PCL concentric ring-banded structures are due to the nonlinear diffusion caused by periodically changing concentration gradient can also be derived from the results obtained at the last stage of spherulite growth. Figure 3d shows the BF image of the boundary of two PCL ring-banded spherulites formed at the solvent evaporation rate of 1.5×10^{-4} mL/h from 5 mg/mL toluene solution at 20 °C. Two inserted white arrows indicate the growth direction of two ring-banded spherulites. As can be seen from Figure 3d,e, the lamellar crystals with the elongated lateral habit in the radial direction and the curved growth faces grow upward and forward and form alternating ridges and valleys of ring-banded structures. At the last stage of spherulite growth, ϕ_0 is approximately the same in different growth period, but ϕ_∞ decreases because of polymer chains exhaustion. Consequently, polymer chains can transport short distances l because of small concentration gradient G. Therefore, the band spacing becomes smaller and smaller, as shown in Figure 3d. There is a gap containing no polymer where ring-banded spherulites come together. The gap results from the polymer chains diffusion because of chains exhaustion in crystals growth front. All the polymer chains had been used up in forming spherulites before the neighboring spherulites grew together.

Fluctuation of polymer solution concentration is inevitable since the actual polymer solution system is not ideal as expounded above. If polymer concentration of the whole solution system increases at some time during the growth of spherulites, polymer chains flux J increases correspondingly with the increase of concentration gradient G. But the crystals growth velocity along the substrate V can be considered changeless. Therefore, inner ring with equal radii, namely wider bands, can be seen from Figure 1. While local fluctuation of polymer solution concentration takes place, the band spacing become large at the area of large concentration gradient G. In other words, the spherulites should grow more rapidly toward the polymer chains abundant source than the other directions. As a consequence, there are

radial irregular features inthe concentric ring-banded spherulites, as shown in Figure 1.

Conclusion

By controlling the solvent evaporation rate, we have obtained concentric ring-banded structures in PCL solution-casting films at the slow solvent evaporation rate. The results indicate that the alternating ridge and valley bands are stacks of lamellar crystals with the polymer chains (*c*-axes) normal to the film plane and growth direction (*b*-axes) coincident with radial direction. A nonlinear diffusion process induced rhythmic growth based on periodically changing concentration gradient in the polymer solution was proposed to explain the formation of the concentric ring-banded structures.

Acknowledgment. The authors thank Prof. Decai Yang at the State Key Laboratory of Polymer Physics and Chemistry of the Changchun Institute of Applied Chemistry for helpful discussions. This work was supported by the National Science Foundation of China (20574068).

References and Notes

(1) Keller, A. *J. Polym. Sci., Polym. Phys.* **1955**, *17*, 351−364.
(2) Xue, M. L.; Shen, J.; Yu, Y. L.; Chuah, H. H. *Eur. Polym. J.* **2004**, *40*, 811−818.
(3) Beekmans, L. G. M.; Hempenius, M. A.; Vancso, G. J. *Eur. Polym. J.* **2004**, *40*, 893−903.
(4) Cheng, T. L.; Su, A. C. *Polymer* **1995**, *36*, 73−80.
(5) Hobbs, J. K.; Binger, D. R.; Keller, A.; Barham, P. J. *J. Polym. Sci., Polym. Phys.* **2000**, *38*, 1575−1583.
(6) Schulze, K.; Kressler, J.; Kammer, H. W. *Polymer* **1993**, *34*, 3704−3709.
(7) Li, W.; Yan, R.; Jiang, B. *Polymer* **1992**, *33*, 889−892.
(8) Singfield, K. L.; Brown, G. R. *Macromolecules* **1995**, *28*, 1290−1297.
(9) Keller, A. *Nature (London)* **1952**, *31*, 913−914.
(10) Keith, H. D.; Padden, F. J. *J. Polym. Sci.* **1959**, *39*, 101−122.
(11) Keller, A. *J. Polym. Sci.* **1959**, *39*, 151−162.
(12) Price, F. P. *J. Polym. Sci.* **1959**, *39*, 139−150.
(13) Ho, R. M.; Ke, K. Z.; Chen, M. *Macromolecules* **2000**, *33*, 7529−7537.
(14) Wang, B. J.; Li, C. Y.; Hanzlicek, J.; Cheng, S. Z. D.; Geil, P. H.; Grebowicz, J.; Ho, R. M. *Polymer* **2001**, *42*, 7171−7180.
(15) Gazzano, M.; Focarete, M. L.; Riekel, C.; Ripamonti, A.; Scandola, M. *Macromol. Chem. Phys.* **2001**, *202*, 1405−1409.
(16) Kyu, T.; Chiu, H. W.; Guenther, A. J.; Okabe, Y.; Saito, H.; Inoue, T. *Phys. Rev. Lett.* **1999**, *83*, 2749−2752.
(17) Keith, H. D. *Polymer* **2001**, *42*, 9987−9993.
(18) Wang, Z.; An, L.; Jiang, B.; Wang, X. *Macromol. Rapid Commun.* **1998**, *19*, 131−133.
(19) Okabe, Y.; Kyu, T.; Saito, H.; Inoue, T. *Macromolecules* **1998**, *31*, 5823−5829.
(20) Chen, J.; Yang, D. C. *Macromol. Rapid Commun.* **2004**, *25*, 1425−1428.
(21) Chen, J.; Yang, D. C. *Macromolecules* **2005**, *38*, 3371−3379.
(22) Duan, Y. X.; Jiang, Y.; Jiang, S. D.; Li, L.; Yan, S. K.; Schultz, J. M. *Macromolecules* **2004**, *37*, 9283−9286.
(23) Duan, Y. X.; Zhang, Y.; Yan, S. K.; Schultz, J. M. *Polymer* **2005**, *46*, 9015−9021.
(24) Wang, Y.; Chan, C. M.; Li, L.; Ng, K. M. *Langmuir* **2006**, *22*, 7384−7390.
(25) Hu, Z. J.; Zhang, F. J.; Huang, H. Y.; Zhang, M. L.; He, T. B. *Macromolecules* **2004**, *37*, 3310−3318.
(26) Schilling, F. C.; Bovey, F. A.; Davis, D. D.; Lovinger, A. J.; Macgregor, R. B.; Walsh, C. A.; Zeigler, J. M. *Macromolecules* **1989**, *22*, 4645−4648.
(27) Nunez, E.; Gedde, U. W. *Polymer* **2005**, *46*, 5992−6000.
(28) Iwata, T.; Doi, Y. *Polym. Int.* **2002**, *51*, 852−858.
(29) Henisch, H. K. *Crystals in Gels and Liesegang Rings*; Cambridge University Press: Cambridge, 1988.
(30) Lauritzen, J. I.; Hoffman, J. D. *J. Res. Natl. Bur. Stand.* **1960**, *64A*, 73−102.
(31) Keith, H. D.; Chen, W. Y. *Polymer* **2002**, *43*, 6263−6272.

MA070334+